

FILED COPY
No. 1

Ames Aeronautical Laboratory
National Advisory Committee
for Aeronautics
Moffett Field, Calif.

6412
54
RT-2

TECHNICAL NOTES

NATIONAL ADVISORY COMMITTEE FOR AERONAUTICS

TN 679

No. 679

NOISE FROM PROPELLERS WITH SYMMETRICAL SECTIONS

AT ZERO BLADE ANGLE, II

By A. F. Deming
Langley Memorial Aeronautical Laboratory

Washington
December 1938

NATIONAL ADVISORY COMMITTEE FOR AERONAUTICS

TECHNICAL NOTE NO. 679

NOISE FROM PROPELLERS WITH SYMMETRICAL SECTIONS

AT ZERO BLADE ANGLE, II

By A. F. Deming

SUMMARY

In a previous paper (Technical Note No. 605), a theory was developed that required an empirical relation to calculate sound pressures for the higher harmonics. Further investigation indicated that the modified theory agrees with experiment and that the empirical relation was due to an interference phenomenon peculiar to the test arrangement used.

Comparison is made between the test results for a two-blade arrangement and the theory. The comparison is made for sound pressures in the plane of the revolving blades for varying values of tip velocity. Comparison is also made at constant tip velocity for all values of azimuth angle β .

A further check is made between the theory and the experimental results for the fundamental of a four-blade arrangement with blades of the same dimensions as those used in the two-blade arrangement.

INTRODUCTION

The effect of blade thickness in producing propeller noise has long been an open question. Only in comparatively recent years has a concerted effort been made to explain fully the general phenomena of propeller noise although it is considered to be the largest contributor to aircraft noise. When the mechanism of propeller rotation noise is fully understood, the possibilities of reducing this noise from its present objectionable level may in some degree be realized.

As the problem of the noise from an actual propeller includes the problem of the present paper, i.e., the thickness effect, it may perhaps contribute to the general understanding of the mechanism of propeller noise. In an actual case of a propeller emitting sound, the paramount effect of the thrust and the torque, in addition to the thickness effect, must be considered. The effect of thrust and torque was treated in a paper by Gutin (reference 1), who limited his paper to natural simplifying assumptions regarding the force distribution on the blade sections.

It was concluded in reference 2 that the theory therein given would render results without undue error only for long wave lengths compared with the propeller diameter. In order to overcome this apparent weakness, an empirical relation was included to obtain correct results for the higher harmonics.

Later examination indicated that the empirical relation could hardly fit the physical picture of sound emanating from the revolving blades. Although at the time of the tests reported in reference 2, the empirical relation was believed to be due to a phenomenon inherent in the source itself, it turned out to be an attempt to make the theory take care of an interference phenomenon inherent in the test set-up. During the present tests, care was taken to avoid interference in the test set-up although measurements of the second harmonic indicated some discrepancy, in that the exponent of V/c did not follow theory; this discrepancy may possibly be due to some interference still persisting in the test set-up.

Besides the consideration of the interference present in the previous tests, an unfortunate error in the calibration of the microphone used introduced an error into the results, which resulted in a statement regarding Gutin's relation that requires correction. In reference 2 it was mentioned that the values of the sound pressures calculated by Gutin's relation were too large. This discrepancy was found to have been overestimated.

The statement made regarding the time-phase relations in reference 2 still remains since the author does not check the 180° phase difference given by Gutin's relation between the azimuth angles of, say, 45° and 135° . Gutin, however, limited his treatment so that consideration of such details as time-phase relations may not be warranted.

According to the literature on propeller-noise investigations, a combination of a microphone, an amplifier, a filter, and a meter has quite often been used. In measurements of this kind, adequate data can be obtained to calculate "loudness" as far as the human ear is concerned but, if the propeller is to be studied as a sound generator, misleading results can thus be obtained. Such an arrangement will, however, give adequate measurements for study of the fundamental if the low-pass filter is properly selected even when the speed is varied. When a filter is used for the study of harmonics, several harmonics are usually included in the filter range and the measurement applies only to the conditions in hand.

The author has experienced misleading results even when dealing with only one harmonic at a time owing to effects that were entirely foreign to both the measuring equipment, which included a frequency analyzer, and the propeller. Such a difficulty gave rise to the empirical relation given in reference 2.

When only the fundamental from a normal-size propeller is dealt with, no foreign effects will usually be experienced but, for harmonics with higher frequencies, serious errors may easily be made, especially when model propellers are considered.

Perhaps it is well to mention another difficulty, which can be very annoying, experienced in making measurements of propeller-rotation noise. This difficulty is mentioned also in references 3 and 4. Gusts of wind may cause the sound pressure to vary considerably. About the only way to obtain a representative value for comparison with theory is to plot a curve through the experimental points and pick a value from the curve.

In reference 2 it was assumed that the "rotation noise" emanated from a narrow ring of mean radius near the blade-tip radius. The present derivation of theory will consider the rotation noise to be generated over the entire disk swept out by the revolving blades and the integration will be so carried out.

DERIVATION OF THEORY

Figure 1 represents the geometry of the problem of rotation noise generated by revolving symmetrical-section blades with zero blade angle. In figure 1, O is the center of the disk described by the revolving blades. In plan view, the axis of the blades is denoted by the line AB, the disk by COD, and the observer's position by P. In elevation view the axis is through O perpendicular to the paper; the disk is denoted by ACBD. An elementary source at dS is shown at a distance R from the center of the disk. As the angle θ is changed continuously, the distance from the observer at P changes periodically by an amount $\pm x$. It is assumed that l is large compared with R.

The blades are of symmetrical section about the chord, have zero blade angle, and operate in quiescent air; a symmetry therefore exists about the plane of the disk. It can be assumed that only one-half the blade, or one side of the chord, is operating and working next to a wall of infinite extent. This fact allows the use of Rayleigh's relation (reference 5) for the potential at a point due to a source in a wall of infinite extent. (If a thrust is exerted, a more general relation would be used giving the potential due to a double source as well.) Rayleigh's relation is

$$\varphi_1 = - \frac{1}{2\pi} \frac{\partial \varphi}{\partial n} \frac{e^{-ikr}}{r} dS \quad (1)$$

where

φ_1 is the velocity potential at any point in question due to source dS.

$\frac{\partial \varphi}{\partial n}$, velocity normal to plane.

r, distance from the elementary source to the point in question.

$$k = \frac{2\pi f}{c} = \frac{2\pi}{\lambda}$$

f, frequency.

λ , wave length.

c , velocity of sound.

dS , area of elementary source.

For the purpose of the problem in hand,

$$\frac{\partial \varphi}{\partial n} = \dot{\xi} = \dot{\xi}_0 [a_n \sin(n\omega t + \epsilon_n) + a_{2n} \sin(2n\omega t + \epsilon_{2n}) \\ + a_{3n} \sin(3n\omega t + \epsilon_{3n}) + \dots + a_{qn} \sin(qn\omega t + \epsilon_{qn}) \\ + \dots] \quad (2)$$

where

$\dot{\xi}_0$ is a parameter proportional to V and dependent on section shape.

n , number of blades.

q , number of harmonics.

a_{qn} , Fourier coefficient.

$\omega = V/R$.

V , velocity of section at radius R .

$dS = R dR d\theta$

ϵ , arbitrary phase angle.

The parameter k can then be written $qn\omega/c$.

Putting the time and space phases for $\partial\varphi/\partial n$ in equation (1),

$$\varphi_{1qn} = - \frac{\dot{\xi}_{qn} dS}{2\pi r} e^{i(qn\omega t + \epsilon_{qn} - qn\theta - kr)} \quad (3)$$

where r is the distance from the elementary source to point P and $\dot{\xi}_{qn} = \dot{\xi}_0 a_{qn}$. Taking into account all the elementary sources dS ,

$$\varphi_{qn} = - \iint \frac{\dot{\xi}_0 a_{qn} e^{i(qn\omega t + \epsilon_{qn} - qn\theta - kr)}}{2\pi r} dS \quad (4)$$

where

$$\begin{aligned} r &= l + x \\ &= l + kR \sin \beta \sin \theta \end{aligned}$$

Inasmuch as x is considered small compared with l , it can be neglected in the denominator with small error but such a procedure cannot be followed in the exponent because there x is a phase factor quite comparable with the wave length λ . Equation (4) is then written

$$\begin{aligned} \varphi_{qn} &= - \int_0^{R_0} \int_0^{2\pi} \frac{a_{qn} \dot{\xi}_0 R e^{i(qn\omega t + \epsilon_{qn} - kl)}}{2\pi l} \\ &\quad \times e^{-i(qn\theta + kR \sin \beta \sin \theta)} dR d\theta \quad (5) \end{aligned}$$

Let

$$M = \frac{a_{qn} \dot{\xi}_0 R e^{i(qn\omega t + \epsilon_{qn} - kl)}}{2\pi l}$$

and

$$m = kR \sin \beta$$

Expanding the exponential in the integral, equation (5) becomes

$$\begin{aligned} \varphi_{qn} &= - \int_0^{R_0} \int_0^{2\pi} M (\cos qn \theta - i \sin qn \theta) \\ &\quad \times \left\{ J_0(m) + 2 \sum_{h=1}^{\infty} J_{2h}(m) \cos 2h \theta \right. \\ &\quad \left. - 2i \sum_{h=1}^{\infty} J_{2h-1}(m) \sin (2h-1) \theta \right\} dR d\theta \quad (6) \end{aligned}$$

This equation integrated from 0 to 2π becomes

$$\varphi_{qn} = (-1)^{qn+1} 2\pi \int_0^{R_0} M J_{qn}(m) dR \quad (7)$$

Since a_{qn} and $\dot{\xi}_0$ in M are functions of R , they must be evaluated in order that the integration with respect to R can be performed. Figure 2 indicates the form of the velocity $\dot{\xi}$ as a blade passes a given point in the path of the blades. As a symmetrical section is considered in this paper, only one side of the section is shown. The actual velocity distribution can be very nearly replaced (at least for the lower-order harmonics) by the triangular distribution shown in figure 2; the positive and the negative areas of this distribution are, respectively, equal to the positive and the negative areas of the actual distribution. In either case, the positive and the negative areas are equal to each other.

It can be readily shown from the Fourier coefficient relation

$$A_g = \frac{1}{\pi} \int_0^{2\pi} f(\alpha) \sin g \alpha d\alpha \quad (8)$$

that the velocity for the q harmonic is

$$A_{qn} \approx \frac{V 2a q n^2 b}{3\pi R^2} \quad (9)$$

where the angle qnb/R is small. It is perhaps convenient to separate A_{qn} into two factors, $\dot{\xi}_0$ and a_{qn} , which were given in equation (2):

$$A_{qn} = \left(\frac{8V a}{3 b} \right) \left(\frac{qn^2 b^2}{4\pi R^2} \right) \quad (10)$$

$$= \dot{\xi}_0 a_{qn} \quad \text{or} \quad V f(a, b) a_{qn} \quad (11)$$

The factor $\dot{\xi}_0$ is the velocity normal to the direction of motion of the section from the head of the blade section

to the maximum ordinate of a diamond-shaped section with the maximum ordinate at the 50-percent-chord position times a factor that takes into account the difference in shape between such a section and the section under consideration. In the present case, the factor is $4/3$ since ξ_0 for the diamond shape described would be $V(2a/b)$. The factor a_{qn} is the Fourier coefficient for a unit rectangular excitation also shown, though not to scale, in figure 2.

Substituting ωR for V ,

$$M = \left(\frac{8}{3} \frac{a}{b}\right) \left(\frac{qn^2 b^2}{4\pi R^2}\right) \frac{\omega R^2}{2\pi l} e^{i(qn\omega t + \epsilon_{qn} - kl)} \quad (12)$$

The thickness ratio a/b is constant over the outer two-thirds of the radius so that, except for the factor b^2 , M may be considered independent of R . The derivation can be simplified by using a representative value of b ; M can then be taken out of the integrand. Of course, b could be considered as a function of R , which it actually is, and the integration performed accordingly. Such complication is hardly warranted unless one is concerned with the higher harmonics; in that case, no simplifying assumptions should be made for the Fourier coefficients.

Since M is thus independent of R , any convenient radius such as the tip radius R_0 may be used in the two factors of M , which have R^2 in the numerator and the denominator. For convenience and so that the final relation will be general in character, equation (12) can be written,

$$M = f(a, b) a_{qn} \frac{\omega R_0^2}{2\pi l} e^{i(qn\omega t + \epsilon_{qn} - kl)} \quad (13)$$

Equation (7) can now be written

$$\varphi_{qn} = (-1)^{qn-1} 2\pi M \int_0^{R_0} J_{qn}(m) dR \quad (14)$$

Since the Bessel function $J_{qn}(m)$ may be expanded as the series

$$J_{qn}(m) = \frac{m^{qn}}{2^{qn}(qn)!} \left\{ 1 - \frac{m^2}{2(qn+2)} + \frac{m^4}{2.4(2qn+2)(2qn+4)} \dots \right\} \quad (15)$$

equation (14) can be integrated to become

$$\begin{aligned} \varphi_{qn} = (1)^{qn+1} 2\pi M R_o \left\{ \frac{m_o^{qn}}{2^{qn}(qn)!} \left(\frac{1}{qn+1} - \frac{m_o^2}{2(qn+2)(qn+3)} \right. \right. \\ \left. \left. + \frac{m_o^4}{2.4(2qn+2)(4qn+4)(qn+5)} \dots \right) \right\} \quad (16) \end{aligned}$$

where $m_o = qn \sin \beta \frac{V_o}{c}$.

The potential φ_{qn} having been obtained at the point P, the sound pressure is readily determined because

$$P_{qn} = -\rho_o \frac{\partial \varphi_{qn}}{\partial t} \quad (17)$$

Equation (16) will, upon differentiation of M with respect to time, become

$$\begin{aligned} p_{qn} = (-1)^{qn} \rho_o qn \omega^2 R_o^2 \frac{R_o}{l} a_{qn} f(a,b) e^{-i(qn\omega t + \epsilon_{qn} - kl)} \\ \left\{ \frac{m_o^{qn}}{2^{qn}(qn)!} \left[\frac{1}{qn+1} - \frac{m_o^2}{2(2qn+2)(qn+3)} + \right. \right. \\ \left. \left. + \frac{m_o^4}{2.4(2qn+2)(2qn+4)(qn+5)} - \dots \right] \right\} \quad (18) \end{aligned}$$

Regrouping the factors in equation (18), noting that $V_o = \omega R_o$, omitting all phase factors, dividing by $\sqrt{2}$ to obtain the root mean square, and multiplying by 2 for ground effect,

$$\begin{aligned} P_{qn} = 2\sqrt{2} qn a_{qn} f(a,b) \frac{R_o}{l} \frac{\rho_o V_o^2}{2} \\ \frac{m_o^{qn}}{2^{qn}(qn)!} \left[\frac{1}{qn+1} - \frac{m_o^2}{2(2qn+2)(qn+3)} + \frac{m_o^4}{2.4(2qn+2)(2qn+4)(qn+5)} - \dots \right] \quad (19) \end{aligned}$$

The sound pressure of the fundamental and of the lower harmonics is thus obtained in terms of the aerodynamic head, the geometry of the arrangement, and the acoustic properties of the medium.

In the calculation of the sound pressures, the following values were used:

Air density ρ , 1.22×10^{-3} grams/cm³.

Ratio of half blade thickness to chord a/b , 0.1.

Blade chord b at $0.80 R_0$, 3.90×2.54 cm.

Blade length to tip R_0 , $4.0 \times 12 \times 2.54$ cm.

Blade tip speed V_0 , cm/sec.

Distance of microphone to center of rotation of blades l , $80 \times 12 \times 2.54$ cm.

Argument of Bessel function, $m_0 = qn \sin \beta V_0/c$,
($\sin \beta = 1.0$).

Velocity of sound c , $1,100 \times 12 \times 2.54$ cm/sec.

A drawing of the blades used in the tests is shown in figure 3.

COMPARISON OF CALCULATED AND EXPERIMENTAL RESULTS

Figure 4 is shown as a typical plot of the logarithm of the sound pressure p_{qn} against the logarithm of V_0/c ; all harmonics to the fifth were similarly plotted and the curves drawn. These curves from experimental data were then all combined on one graph together with the curves calculated from equation (19) and are shown in figure 5.

The mean slope of the curves of figure 5 is plotted against qn in figure 6. If the sound were assumed to come from a narrow ring, as stated in reference 2, the solution would contain $J_{qn}(m)$. In such a case, the slopes or exponent would be somewhat greater, as also shown in

figure 6. In reference 2 the factor K was 0.80, but a factor of 0.85 would have checked the results of figure 6 more closely.

POLAR DISTRIBUTION OF SOUND PRESSURE

The sound pressures in percentage of the value at $\beta = 90^\circ$ of the first four harmonics for the two-blade arrangement are plotted in polar coordinates, which show the distribution about the disk traversed by the blades. The axis of rotation is taken as the reference axis with the front of the driving motor as the zero direction. The polars are plotted in figure 7 with the continuous lines representing the experimental values and the dashed lines the calculated distribution. All data on these polar graphs are for a constant speed of 1,780 r.p.m. The values of sound pressure at $\beta = 90^\circ$ may be taken from figure 5.

COMPARISON BETWEEN MEASURED AND CALCULATED SOUND

PRESSURE FOR A FOUR-BLADE ARRANGEMENT

As a further check, comparison was made between experimental and calculated results for a four-blade arrangement. The four blades used were equally spaced and were all of the same size and shape as the blades of the two-blade arrangement except up to $1/3 R_0$.

Owing to flutter, the top speed obtained with the four-blade arrangement was less than that obtained with the two-blade arrangement because the four-blade arrangement is less stiff in transverse and torsional flexure. A reasonable speed range was used, however, in which theory and experiment agreed to about 1 db for the fundamental (fig. 8). In general, with rotation noise, the higher harmonics appear at higher values of V_0/c ; in this case of the four-blade arrangement, the second harmonic was of too low a level to get adequate data owing to the low values of V_0/c used. It may be added, however, that the only experimental point taken of the second harmonic did check fairly well with the theory.

DISCUSSION

It will be seen that the slopes in figure 5 or the exponents in figure 6 as experimentally obtained for the second harmonic are greater than the theory indicates. This difference may be due to an interference phenomenon peculiar to the wave-length range of the second harmonic still persisting in the set-up. In this case the experimental value of the slope is greater than the theory indicates; whereas, in the results reported in the preceding paper (reference 2), it was less.

It has perhaps been noted that the discrepancy between theory and experiment, as shown on figure 5, indicates a trend from the fundamental to the fifth harmonic, i. e., the discrepancy becomes less as higher harmonics are considered and the discrepancy may even change sign if harmonics higher than the fifth are considered. Apparently the factor q does not have quite the effect the theory indicates. It must be remembered that q is contained in a_{qn} , which as calculated becomes of questionable value as the harmonics of the order of $2\pi R/nb$ are approached.

It will be noticed in figure 7 that the sound pressure on the axis is not zero as given by the theory. This discrepancy is very probably due to the fact that the blades do not operate in free space and are not free of obstructions, as assumed in the theory. The peak just ahead of the 90° position shown by the experimental curves for the fundamental and the second harmonic may be due to a slight twist of the blades. For propellers exerting thrust, the polar curves for the fundamental and the second harmonic give a maximum usually about 30° behind the plane of rotation in the direction of the velocity of air through the blade disk.

CONCLUSIONS

1. The theory gives the sound pressure with fair accuracy for the purpose for the first five harmonics of a two-blade arrangement with symmetrical sections exerting zero thrust for values of V_0/c up to 0.80. It may even be said that the theory appears general enough to give fair results for harmonics of the order of $\frac{1}{2}(2\pi R/nb)$ (one-half the r

half the reciprocal of the solidity at $0.80 R_0$) for values of V_0/c up to 0.80.

2. The effect of blade thickness of propellers alone in producing noise is small except for low angles of attack; that is, the rotation noise of a propeller producing normal thrust gives sound pressures larger than measured in these tests where only thickness effect was involved and where the thickness was larger (0.20) than the thickness for the outer sections of a normal propeller.

3. A relationship has been derived that gives the shape of the polar distribution of rotation noise for the first four harmonics fairly well within the speed range used.

Langley Memorial Aeronautical Laboratory,
National Advisory Committee for Aeronautics,
Langley Field, Va., September 12, 1938.

REFERENCES

1. Gutin, L.: ^UÜber das Schallfeld einer Rotierenden Luftschraube. Physikalische Zeitschrift der Sowjetunion, vol. 9, no. 1, 1936, pp. 57-71.
2. Deming, A. F.: Noise from Propellers with Symmetrical Sections at Zero Blade Angle. T.N. No. 605, N.A.C.A., 1937.
3. Obata, Juichi, Yosida, Yahei, and Yosida, Umeziro: On the Directional Properties of Airscrew Sound. Report No. 134 (vol. XI,2), Aero. Res. Inst., Tokyo Imperial Univ., Feb. 1936.
4. Obata, Juichi, Kawada, Sandi, Yosida, Yahei, and Yosida, Umeziro: On the Relation between the Performance and the Loudness of Sound of an Airscrew. Report No. 141 (vol. XI,9), Aero. Res. Inst., Tokyo Imperial Univ., July 1936.
5. Rayleigh, Lord: The Theory of Sound. Vol. II. Macmillan & Co., Ltd. (London), 1878 (reprint of 1929).

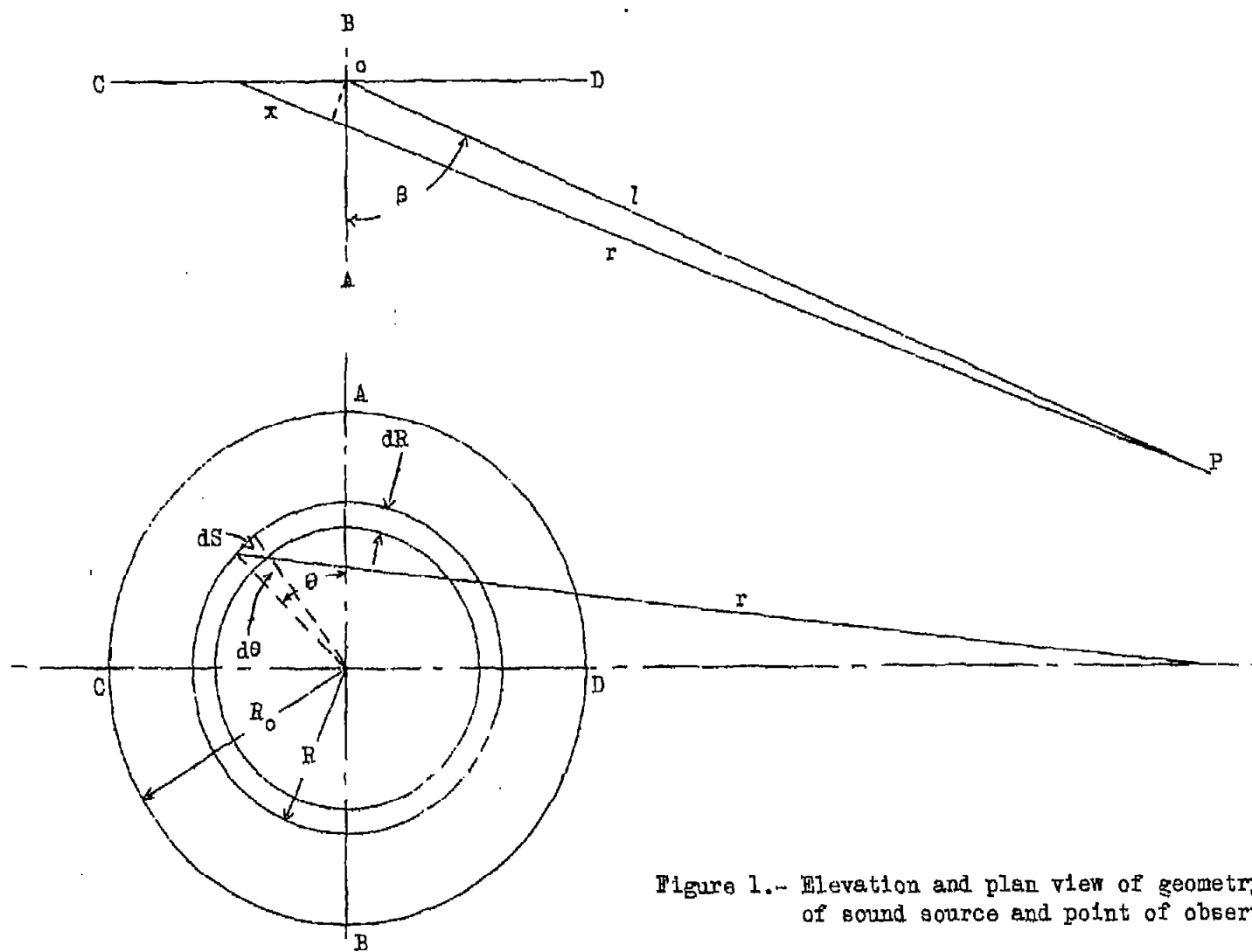


Figure 1.- Elevation and plan view of geometry of sound source and point of observation.

E R R A T A

NATIONAL ADVISORY COMMITTEE FOR AERONAUTICS

TECHNICAL NOTE NO. 679

NOISE FROM PROPELLERS WITH SYMMETRICAL SECTIONS

AT ZERO BLADE ANGLES, II

Figure 6: The reference in this figure should read
"reference 2" instead of "reference 1".

The function " $J_{qn} \left(qnk \frac{V_0}{c} = 0 \right)$ " should read

" $J_{qn} \left(qnk \frac{V_0}{c} \right)$ ".

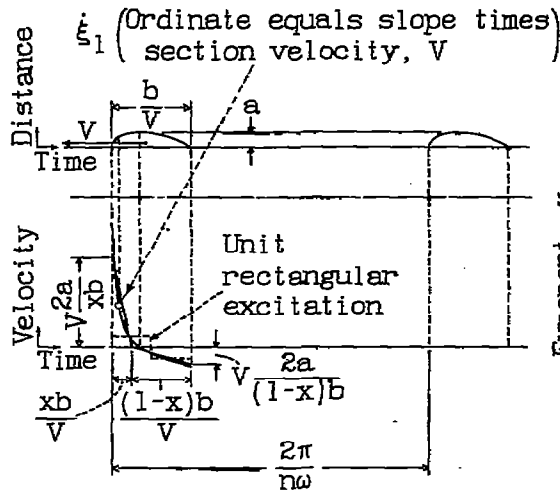


Figure 2.- Source velocity, ξ

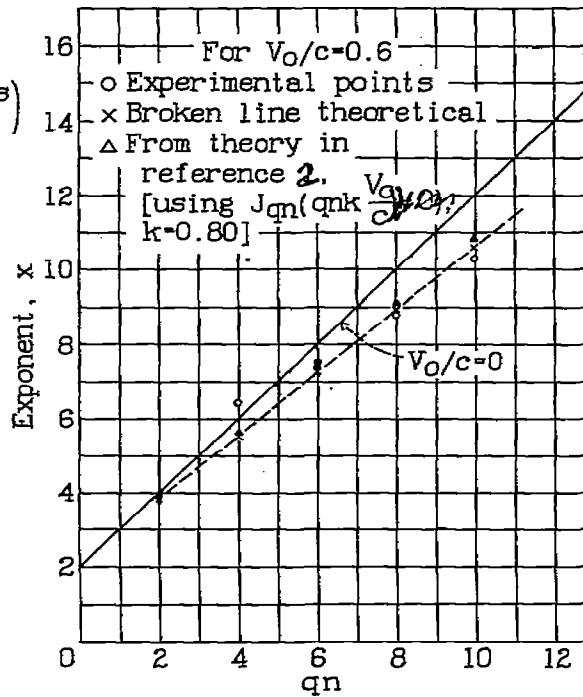


Figure 6.- Exponents of V_0/c against qn .

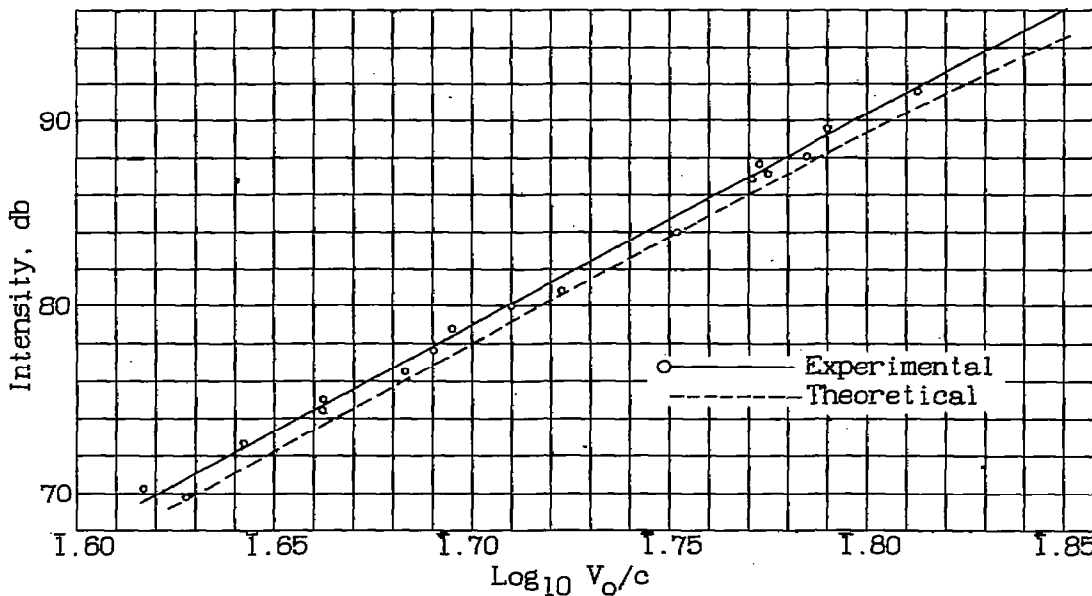
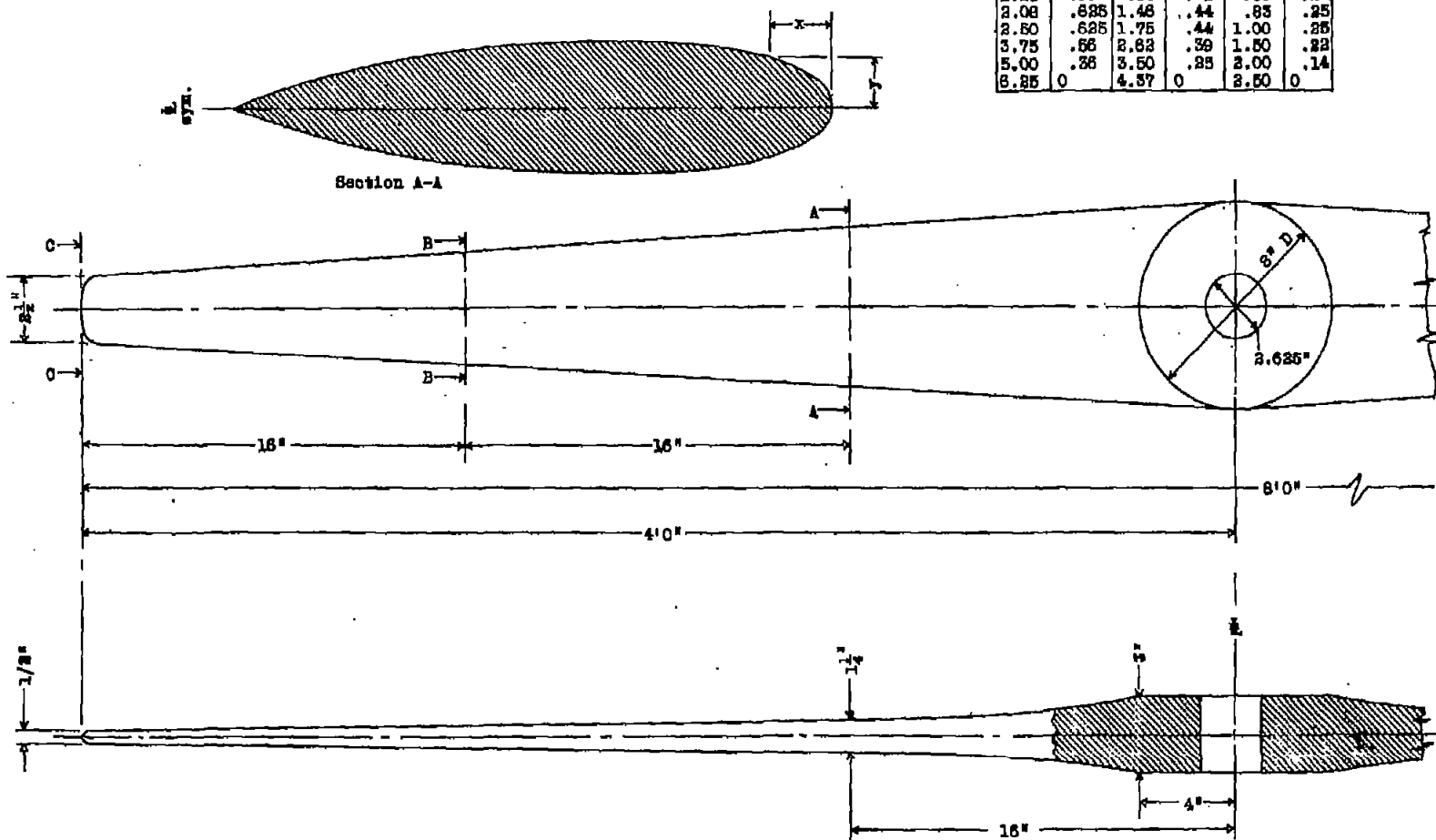


Figure 8.- Intensity in decibels of the fundamental for a four-blade arrangement against $\log_{10} V_0/c$

Dimensions of sections (in.)

| Sec. A-A | | Sec. B-B | | Sec. C-C | |
|----------|------|----------|------|----------|------|
| x | y | x | y | x | y |
| 0.82 | 0.48 | 0.44 | 0.34 | 0.25 | 0.19 |
| 1.25 | .59 | .88 | .41 | .50 | .34 |
| 2.08 | .685 | 1.48 | .44 | .83 | .35 |
| 2.50 | .685 | 1.75 | .44 | 1.00 | .35 |
| 3.75 | .68 | 2.62 | .39 | 1.50 | .22 |
| 5.00 | .38 | 3.50 | .25 | 2.00 | .14 |
| 6.85 | 0 | 4.37 | 0 | 2.50 | 0 |



Symmetrical section; material, spruce; blade angle, zero.

Figure 3.- Blades used in sound tests.

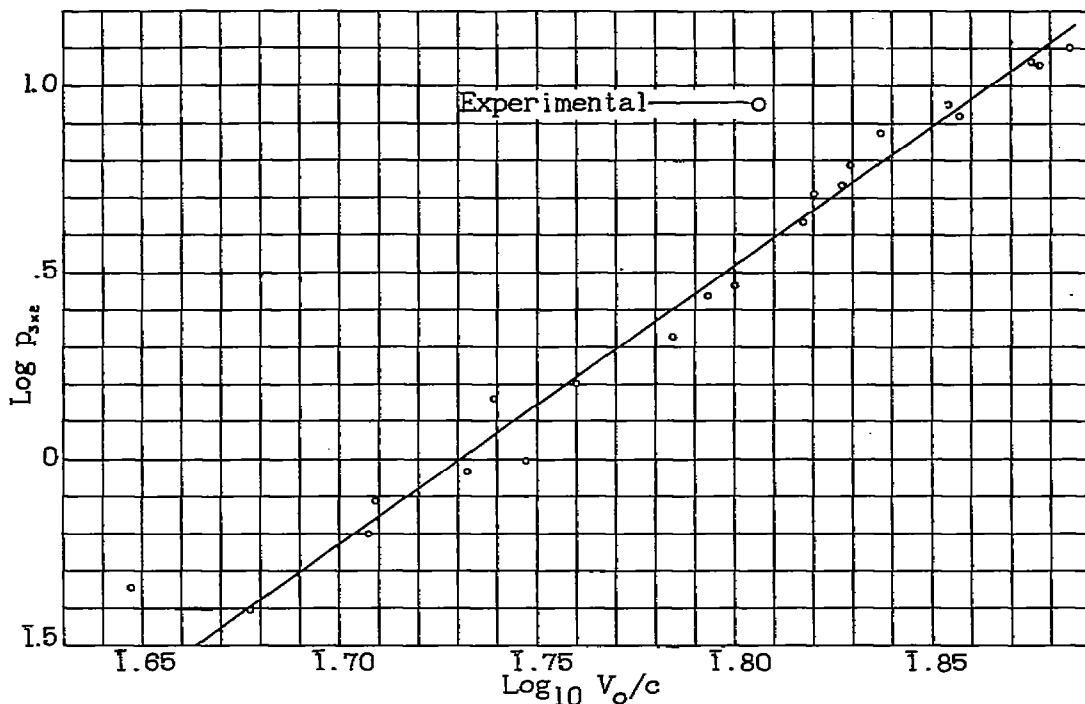


Figure 4.- Typical graph of logarithm of sound pressure against $\text{Log}_{10} V_0/c$.

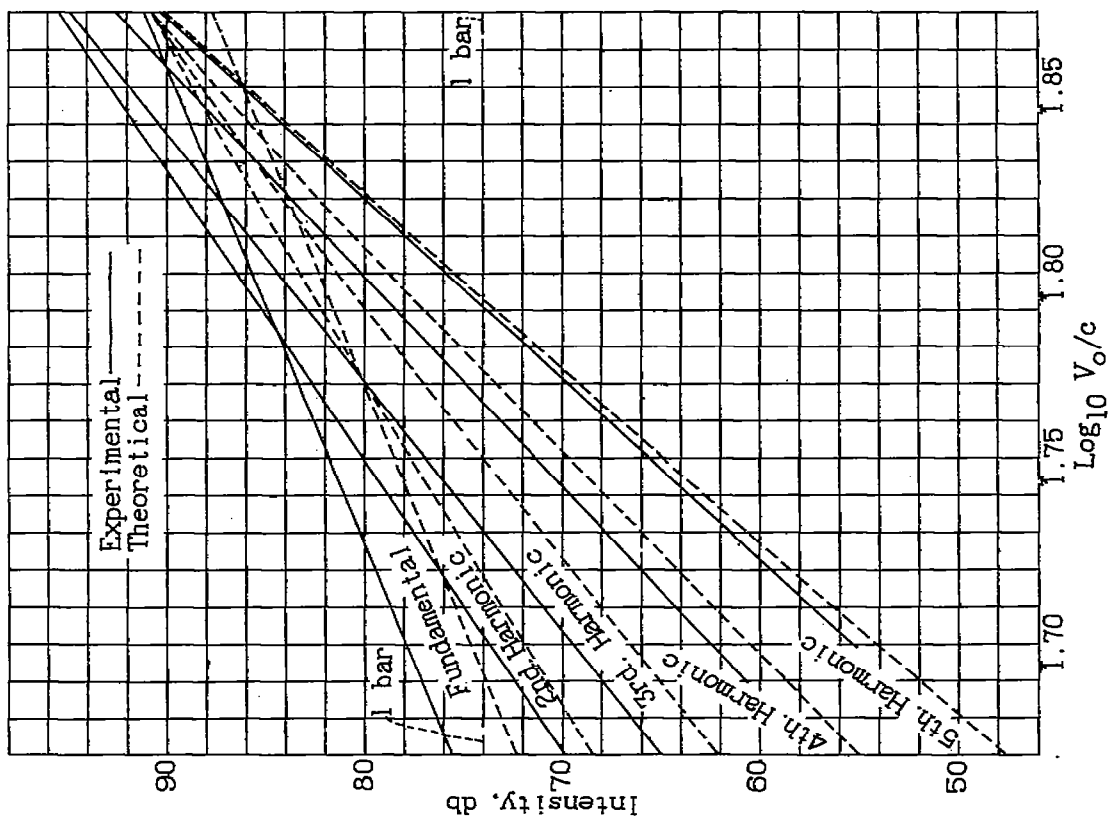
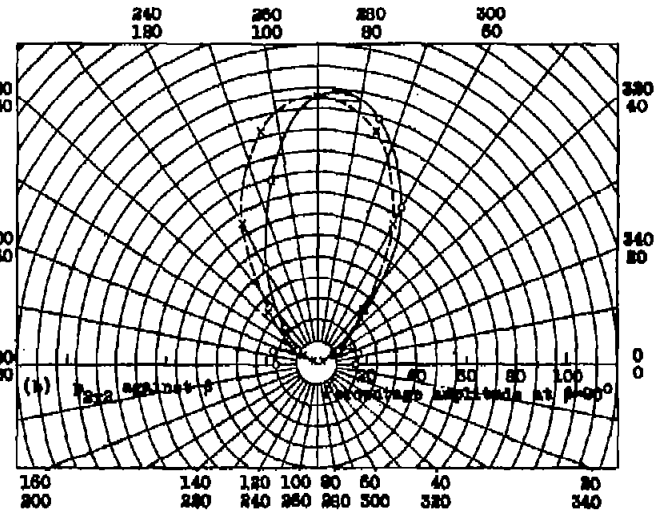
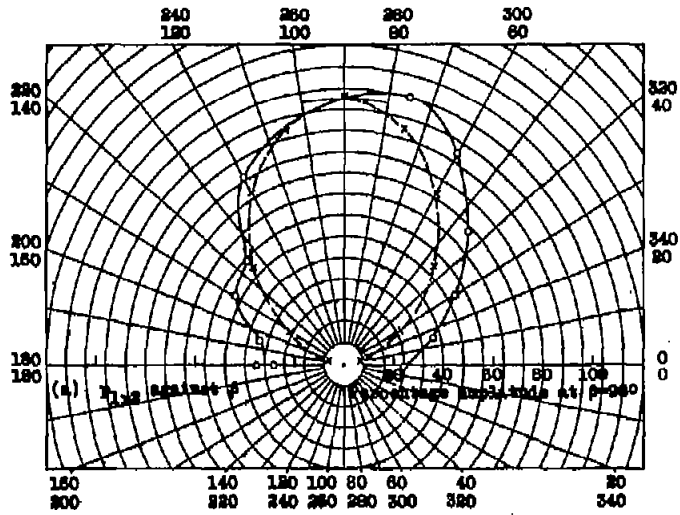


Figure 5.- Intensity against $\text{log}_{10} V_0/c$



—○— Experimental
- - - x - - - Theoretical

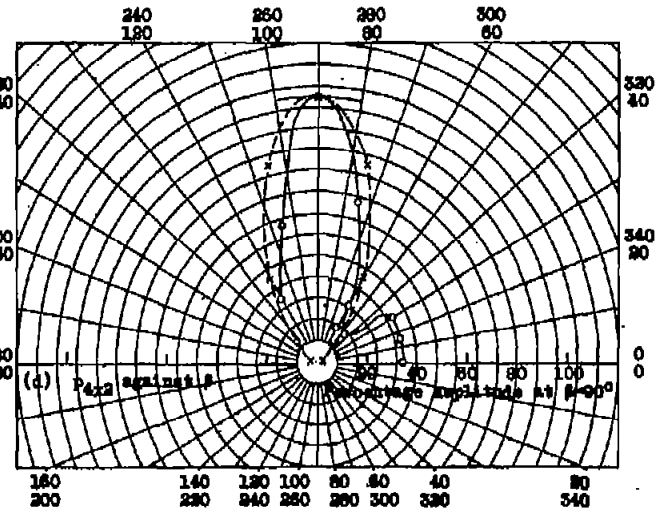
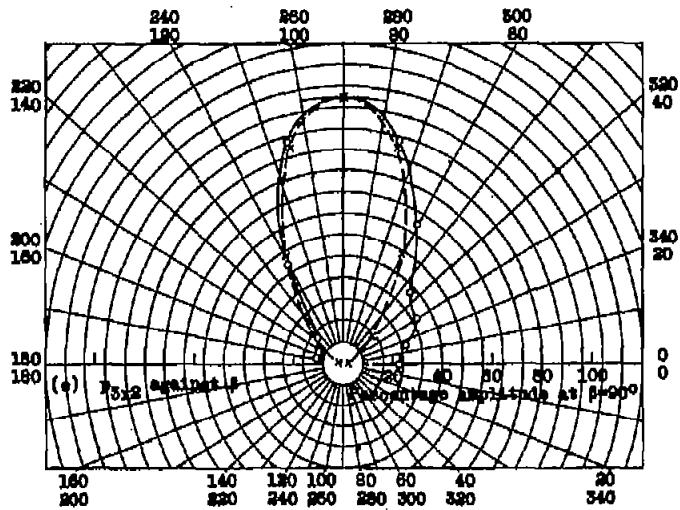


Figure 7a,b,c,d.- Sound pressure against β for the first four harmonics.